THE JOURNAL OF PHYSICAL CHEMISTRY A

ARTICLE

pubs.acs.org/JPCA

Characterization of Low-Frequency Modes in Aqueous Peptides Using Far-Infrared Spectroscopy and Molecular Dynamics Simulation

Tao Ding,[†] Thomas Huber,[‡] Anton P.J. Middelberg,[†] and Robert J. Falconer*[,§]

[†]Australian Institute for Bioengineering and Nanotechnology, The University of Queensland, Brisbane, Australia

[‡]Research School of Chemistry, Australian National University, Canberra, Australia

[§]Department of Chemical and Biological Engineering, ChELSI Institute, University of Sheffield, Sheffield S1 3JD, England

Supporting Information

ABSTRACT: Far-infrared spectroscopy was used to study the dynamics of three aqueous peptides having varied helicity. Experimental data were compared to the molecular dynamics simulated far-infrared absorbance spectrum derived from the dipole time correlation function. Vibrational density of state (VDOS) simulation was then used to analyze the contribution of different structural elements to the bands. Frozen aqueous peptide samples were studied in the frequency range between 325 and 540 cm^{-1} where the ice absorbance is low. Three resonances were identified; band I centered at approximately 333 cm^{-1}, band II centered at approximately 380 cm^{-1}, and band III comprising two constituent bands at approximately 519 and 528 cm^{-1}. The peak height and frequency of the maximum absorbance of bands I and II varied depending on the helicity of the peptide. VDOS of the far-infrared absorbance spectrum confirmed that bands I and II were associated with the peptide backbone and that band III had both potential backbone and side chain components.

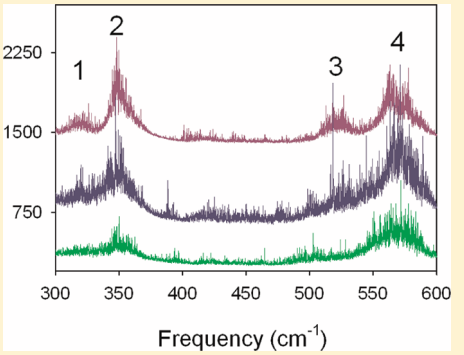

INTRODUCTION

Proteins play a central role in cell biology and are becoming an increasingly significant family of molecules for pharmaceutical intervention. Consequently, analysis of these macromolecules is of increasing importance to study their physiological functionality and guarantee structural and functional integrity in therapeutic formulations. Noninvasive optical methods have been developed to study the native conformation of the biomolecules in aqueous solution using circular dichroism (CD) spectroscopy[1,2] and vibrational spectroscopy using mid-infrared (IR) radiation.[3−6] Terahertz and far-infrared spectroscopy has had less application due to the technical difficulties of working in this part of the electromagnetic spectrum. Terahertz and far-infrared spectroscopy, however, provide a potential means of studying low-frequency molecular motions within a macromolecule and offer an alternative route to structural understanding.

Early far-infrared spectroscopy studies on polyamides and proteins have provided some insight into low-energy resonances in these systems. Studies using pure N-methylacetamide (the simplest molecule with a peptide bond) have bands at 120 cm^{-1} assigned to CO···HN intermolecular hydrogen bonding and at 201 cm^{-1} assigned to C−N torsional vibration of the peptide bond. Studies of polyamides went further to assign absorbance peaks below 600 cm^{-1} to intermolecular hydrogen bonding vibrations, methyl and C−N torsional vibrations, and α-helices.[7−12] Proteins, unlike polyamides, have broad spectral features, one centered on 150 cm^{-1} with smaller features around 320 cm^{-1}, which are currently difficult to interpret.[13] This demonstrates the potential of far-infrared spectroscopy for some primary and secondary structural analysis of peptides and proteins. More recent studies have illustrated the potential of far-infrared spectroscopy for protein quaternary structural analysis. This has revealed markedly different absorbance spectra for the polyomavirus capsid protein before and after assembly,[14] though spectral differences (between 50 and 350 cm^{-1}) associated with lysozyme fibril assembly could be accounted for by Rayleigh light scattering.[15] Terahertz time-domain spectroscopy of protein between 3 and 100 cm^{-1} demonstrated a monotonic increase in absorbance as the frequency increased and that light scattering has to be considered when interpreting the results.[15,16]

Sample preparation is important if far-infrared spectroscopy is to yield useful results. Pioneering studies on cast films proved the existence of spectral features for peptides,[13] however it can be difficult to preserve the native structure for biomolecules under these conditions. Drying methods such as lyophilization may induce secondary structural change or aggregation and should be avoided if possible.[17,18] Sample preparation that maintains conditions as close as physiological for the protein has obvious merit.

Interpretation of far-infrared spectral features can be aided with the use of molecular dynamics (MD) simulation.[19−21] MD

Received: January 18, 2011
Revised: September 12, 2011

   dx.doi.org/10.1021/jp200553d | J. Phys. Chem. A XXXX, XXX, 000–000

Table 1. Amino Acid Sequence and Helicity of AK17, AK10G, and AK9P at 298 K[a]

name	amino acid sequence	helicity (%; measured by CD)
AK17	AC-AKAAAAKAAAAKAAAAK-NH_2	72.4
AK10G	AC-AKAAAAKAAGAKAAAAK-NH_2	29.5
AK9P	AC-AKAAAAKAPAAKAAAAK-NH_2	0.0

[a] A, alanine; K, lysine; G, glycine; P, proline.

is able to access dynamical properties of the molecule at a finite temperature, intrinsically including the solvent effects and the experimental averages can be achieved through sufficient time sampling.[22] In previous studies, ab initio MD schemes have been employed.[23] The total size of our molecular system with peptide and surrounding water makes this approach impractical. For this reason, a classical MD scheme and semiempirical potentials were chosen to simulate low-energy resonances in the peptides of interest. In this study we studied a group of three closely related peptides with known helicity (Table 1). A FTIR spectrometer with a liquid-helium-cooled bolometer and a synchrotron light source was used to measure the absorbance of each peptide. Samples were prepared as pressed pellets of lyophilized protein or as aqueous preparations, both cooled to 79 ± 1 K. The aim of the work was to determine whether far-infrared spectroscopy can identify α-helical secondary structures in peptides and whether MD can be used to interpret observed resonances.

2. MATERIALS AND METHODS

2.1. Sample Preparation. Three alanine-rich peptides were chemically synthesized with higher than 95% purity (Mimotopes, Clayton, Australia). The amino acid sequences of these three peptides (AK17, AK10G, and AK9P) are provided in Table 1. AK17 is comprised of multiple repeats of four alanine residues followed by a lysine residue and has predictable α-helical structure. AK10G differs from AK17 by one glycine residue that was substituted at the 10th position to partially perturb the α helix. AK9P differs from AK17 by one proline residue that was substituted at the ninth position, where it causes a major perturbation of the α-helical structure.

The buffer used in this study (KF buffer) comprised 100 mM potassium fluoride, 1 mM potassium phosphate buffer, pH7. The 100 mM peptide in KF buffer and buffer reference samples (6 μL) were placed between two 1 mm thick polypropylene (PP) windows (Goodfellow, U.K.) using a 170 μm thick PP spacer, clamped in position between two copper plates with a 10 mm aperture. Three sample holders were clamped onto the cryostat coldfinger ready for analysis. The spectra of dry peptide were measured using pressed pellet containing 10 mg of peptide lyophilized powder mixed with 30 mg of Uvasol photometric grade polyethylene (Merck, Germany), pressed as 13 mm diameter discs, with 7 tonne-force for 3 min. The pellets were clamped into the cryostat coldfinger ready for analysis.

2.2. Secondary Structure Characterization by Circular Dichroism Spectroscopy. Circular dichroism was measured with a circular dichroism spectrometer (J-815, Jasco Tokyo, Japan) and a 10 mm path length cell. The three peptides were dissolved in KF buffer at 100 μM peptide concentration and all measurement were conducted at 273 K. The percentage of helicity was estimated from the θ_{222} value.[24]

2.3. Far Infrared Spectroscopic Measurement Using a Synchrotron Light Source. Far infrared spectroscopic measurements were performed on the far-infrared and high resolution FTIR beamline at the Australian Synchrotron (Clayton, Victoria) operating at 3 GeV and a maximum current of 200 mA. The beam dimension was 480 μm (horizontal) by 13 μm (vertical), the opening angle collected was 50 (horizontal) by 16 mrad (vertical). The beam was a converging source close to a point. The sample was mounted in a Janis ST-100 FTIR cryostat (Wilmington, MA, USA) coldfinger and cooled with liquid nitrogen to 78 K. The temperature of the coldfinger was measured using a temperature controller (331S, Lake Shore, Westerville, OH, U.S.A.). Transmission spectra were recorded using a Bruker IFS 125HR Fourier Transform Infrared spectrometer (Bruker Optics, Ettlingen, Germany) fitted with a 6 μm Mylar multilayer beam splitter, scanner velocity of 40 kHz, and a liquid helium-cooled Si bolometer detector with aperture setting of 4 mm. Each spectrum was an average of 26 scans recorded with the maximum frequency limit of 700 cm^{-1} and at a resolution of 0.25 cm^{-1}. To eliminate the etalon effect due to reflection of the measurement cell, a Tukey window with apodization function[25] was applied to all interferograms prior to fast Fourier transformation. A sample cell containing KF buffer was used as the reference for the aqueous peptide samples and pure polyethylene pellets were used as the reference for the lyophilized peptide samples.

2.4. Data Evaluation. The three main band regions (denoted I−III) in the absorption spectra of aqueous sample were initially identified by means of second derivative method in OPUS 6.0 software (Bruker Optics, Ettlingen, Germany). To avoid interference with bands I−III, eight frequencies points of 325, 350, 400, 425, 450, 475, 500, and 540 cm^{-1} were used to define the baseline, which was subsequently subtracted from the absorption spectra. Identical baseline treatment was applied to all aqueous absorption spectra in this study. For measuring the band intensity and band position, a least-squares curve fitting method was applied to all baseline corrected spectra. The band positions resulted from this evaluation process and those with those generated from OPUS analysis agreed well, differing by less than 1 cm^{-1}.

2.5. Molecular Modeling and Molecular Dynamics Simulation. Molecular dynamics simulations were performed with the GROMACS 3.3.2 package.[26] The peptide models were generated by Modeler as α-helical configurations. The molecules were "dissolved" in a simulation box of SPC[27] (single point charge, a three-point model for water), the minimum distance between solute and the edge of box was set to 1.2 nm (equivalent to a concentration of approximately 20 mM). GROMOS 45A3 force field[28] and NPT conditions (number of particles, system pressure, and temperature (T = 273 K) held constant) were used for each peptide. A twin-range cutoff scheme with 0.8 and 1.4 nm cut-off radii was applied, in which interactions within the shorter range cut off (0.8 nm) were calculated every step, whereas interactions within the longer cut off (1.4 nm) were updated every five steps, together with the pair list. The time step was 2 fs and nonbonded interactions in the range between these radii were updated every fifth time step. A total of 6 ns of simulations were performed prior to 1 ns of sampling period, atomic trajectories were sampled every 20 fs.

The simulated far-infrared absorbance spectrum was derived from the dipole time correlation function (TCF). The TCF is obtained in a molecular dynamics simulation described above. The IR spectrum of AK17 was calculated based on the Fermi Golden Rule formula, which is commonly rewritten as Fourier

dx.doi.org/10.1021/jp200553d |J. Phys. Chem. A XXXX, XXX, 000–000

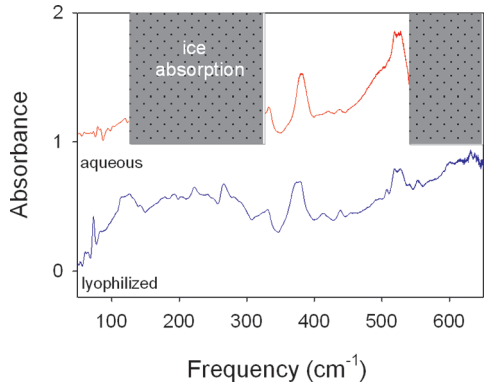

Figure 1. Absorption spectrum of AK17 prepared as aqueous frozen and dry lyophilized samples. Both measurements were conducted at 78 K: red, absorbance of 100 mM AK17 peptide in solution relative to buffer; blue, absorption of 10 mg AK17 lyophilized powder relative to blank PE pellet. For clarity, absorption of aqueous offset upward by 1.0 A.U.

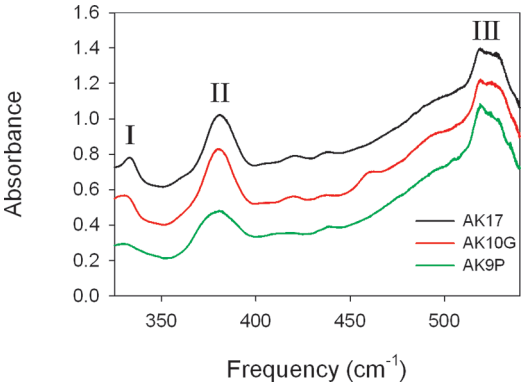

Figure 2. Absorption spectrum of 100 mM peptide in solution from 325 to 540 cm^{-1}, measured at 78 K, relative to buffer: black, AK17; red, AK10G; green, AK9P. For clarity, absorption of AK10G and AK17 are offset upward by 0.2 and 0.4 absorbance units, respectively. Strong absorption bands are labeled as I, II, and III.

transform of the TCF.[29] The formula used is described in eq 1.

$$a(\omega)n(\omega) = \frac{2\pi\beta\omega^2}{3cV}\int_{-\infty}^{+\infty}\langle M(t)M(0)\rangle e^{iwt}\mathrm{d}t \qquad (1)$$

where $\alpha(\omega)$ is the frequency dependent absorption coefficient, n is frequency dependent reflective index, $\beta = 1/kT$, c is the speed of light in vacuum, and V is the volume. The angular brackets denoted the statistical average of the correlation of dipole moment M of the peptide molecule, which is defined by the force field model.

Vibrational density of state (VDOS) simulation of the far-infrared absorbance spectrum reflects the overall dynamic of a molecular system. It was obtained by the Fourier transformation of the autocorrelation of time-dependent atomic velocity.[30]

$$\mathrm{VDOS}(\omega) = \sum_{i=1,N}\int_{-\infty}^{\infty}\langle v_i(t)\cdot v_i(0)\rangle \exp(i\omega t)\mathrm{d}t \qquad (2)$$

$v_i(t)$ is the velocity of atom, and i and N are the total number of atoms in the system. The VDOS can be decomposed into subgroups of atom by restraining the sum over i in eq 2.

3. RESULTS

3.1. Optical Measurements Using Synchrotron FTIR. The peptide samples were prepared in two ways; as pressed pellets of lyophilized peptide mixed with polyethylene powder or as frozen samples of peptide dissolved in KF buffer. The aim was to determine whether lyophilized peptide was suitable for generating a useful far-infrared absorbance spectrum or whether the peptide in a frozen aqueous medium was superior for far-infrared analysis. Transmission measurements were taken with samples at 78 K using a FTIR spectrometer equipped with a Mylar multilayer beam splitter, a liquid helium-cooled Si bolometer, a cryostat sample holder and a synchrotron light source.

The aqueous peptide samples had two strong ice absorption bands centered at approximately 230 cm^{-1} and 850 cm^{-1}.[31] This limited the usable spectral bandwidth to 50−120 and 325−540 cm^{-1} (Figure 1). The usable spectral bandwidth of the lyophilized samples was not affected by ice absorbance and was usable between 50 and 600 cm^{-1}. The absorption characteristics of the peptides in the common region between 325 and 540 cm^{-1} followed a similar pattern for both the lyophilized and aqueous peptide samples.

The far-infrared absorbance spectra for the three aqueous peptide samples between 325 and 540 cm^{-1} had a positive absorbance across the whole frequency range, which indicated stronger absorption of the peptide material compared to its counterpart ice (Figure 2). Three major absorption bands were observed within the available bandwidth (denoted I, II and III). Band I was centered at 333 cm^{-1} for AK17, the peak height was diminished in AK10G samples and nearly disappeared for AK9P. Band II is a very prominent band centered at approximately 380 cm^{-1} for AK17 samples. This band shows similar intensity and position for AK10G but absorbance diminished in the AK9P sample. Band III is strong and relatively wide band that possess a complex structure with two constituent bands at approximately 519 cm^{-1} and 528 cm^{-1}. The absorption level of band III is very similar for the three peptides.

Far-infrared spectra were generated for the three peptides prepared as pressed pellets of lyophilized peptide mixed with polyethylene (Figure 3A). For both AK17 and AK10G, the aqueous and dried peptides spectra are quite similar (Figures 2 and 3A). Comparison of the lyophilized peptide with the aqueous samples (Figure 3B) revealed a red-shift in bands I and II of approx 5 cm^{-1} between the aqueous and lyophilized peptide spectra. The relative intensity between these two bands also remained similar between aqueous and lyophilized peptide measurements. While lyophilization is effective at removing the water from a peptide sample it is known to alter the structure of proteins.[17,18] Lyophilized AK17 and AK10G spectra were very similar, indicating that both peptides may have assumed a helical structure on drying. Lyophilized AK9P spectrum was radically different to its aqueous spectrum, band I was diminished in both spectra, band II had all but disappeared and band III had changed from a broad double peak to a narrower single peak. It was also radically different to the spectra of lyophilized AK17 and AK10G. Interestingly, we observed a prominent double peak centered at 440 cm^{-1} in the lyophilized AK9P spectrum (Figure 3A), which is absent from the aqueous sample. This band at 440 cm^{-1} has previously been documented for the β-form of L-polyalanine analyzed as a dry material,[13,32] indicating that AK9P may be forming β-pleated sheets during the lyophilization process. Interaction between the polyethylene and peptide is also a possible mechanism

dx.doi.org/10.1021/jp200553d |J. Phys. Chem. A XXXX, XXX, 000–000

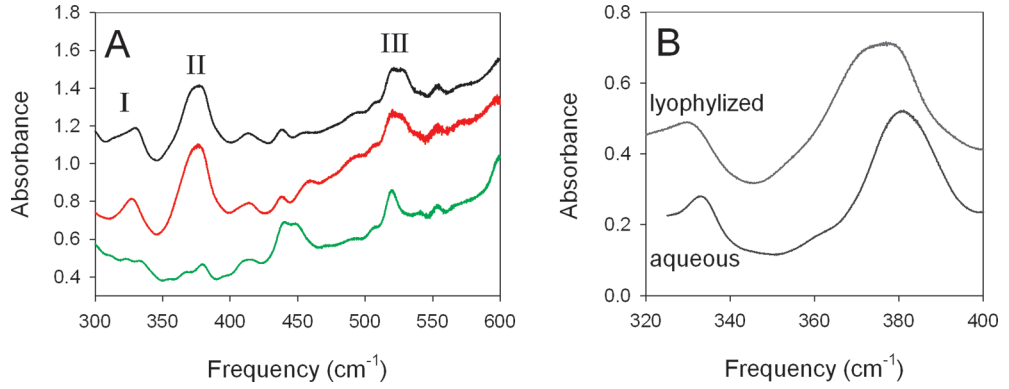

Figure 3. (A) Comparison of peptide absorption spectra measured as lyophilized peptide, 300−600 cm^{-1} is shown: black, AK17; red, AK10G; green, AK9P. The AK17 spectra are offset upward by 0.6 A.U for clarity. (B) The comparison of freeze-dried and aqueous spectra of AK17 in the frequency range of 320−400 cm^{-1}, both measured at 78 K.

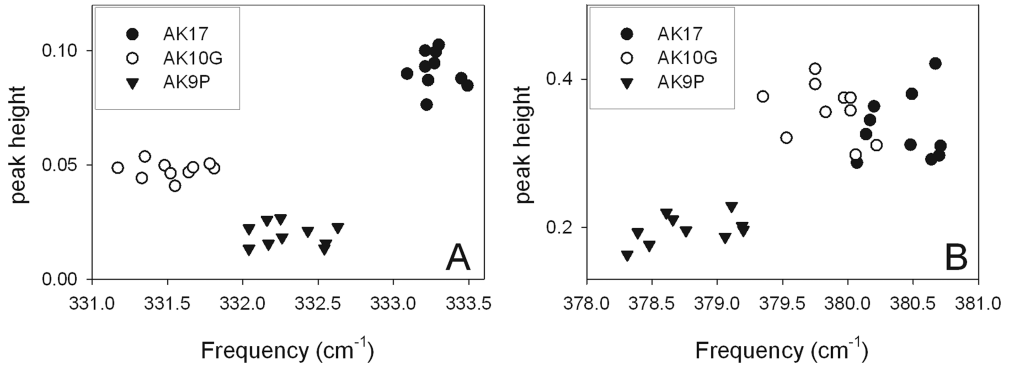

Figure 4. Peak height and frequency of the maximum absorbance for (A) bands I and (B) II of peptide in solution (refer to Figure 2). All absorbance measurements were conducted at 78 K.

for altering the spectrum though the authors believe this is unlikely. The aqueous sample preparation was selected for further experimentation based on the lack of obvious evidence of secondary structural change during sample preparation.

The relationship between the far-infrared spectrum and peptide helicity was investigated by looking for variations in band position and absorbance for bands I and II derived from aqueous peptide samples (Figure 4). The peak height represents the maximum absorbance mapped after baseline correction and the frequency is the position with maximum absorbance. Ten individual measurements were made for each peptide. Very clear separation was observed in the three peptides for band I (Figure 4A) where shifts in both band peak height and frequency were apparent. The band absorbance displays a gradual change in the order of AK17 > AK10G > AK9P, which corresponds to the same order as their helicity determined by circular dichroism spectroscopy (Table 1). The very weak band I with low peak height for the random coil peptide AK9P suggests the dominance of structural related vibrational mode(s) in this band. For band II, AK17 and AK10G shared very similar band absorbance and frequency (Figure 4B). However, clear separation was observed between the random coil peptide AK9P and the other two peptides, both in terms of band absorbance and frequency. In contrast to band I, reasonable amount of band absorbance remained for AK9P, suggesting only a small portion of the modes contributing to this band are associated with helicity and random coil structure retains some absorbance at 380 cm^{-1}. An alternative explanation may be that freezing of the peptide solution promoted α helix formation leading to a little helical content in AK9P and helical content in AK10G similar to AK17. This may explain the discrepancy between the room temperature circular dichroism measurements (Table 1) and the 78 K far-infrared observations for bands I and II (Figure 4).

3.2. Calculation of the IR Spectrum and VDOS of the Peptides Using Molecular Dynamics Simulation. The three peptides in this study display substantial variations in absorption features despite very similar chemical composition. A significant amount of spectral difference appears to depend on the secondary structure. This phenomenon represented an interesting case for molecular dynamics (MD) based simulation study, in which peptide molecular dynamics and anharmonicity introduced by the solvent environment are reproduced in the calculation. The molecular dynamic simulation package GROMACS was used to construct an α-helical model of AK17 which was used in the classical MD simulation of the IR spectrum (see Materials and Methods for details). For ribbon diagrams of the peptide conformations see Ding et al. 2010.[33] During the MD simulation, the temperature was kept at 298 K using semiempirical force fields parametized at room temperature. Experimental observation justifies this decision as the spectra of dried peptide at 78 and 298 K were very similar (data not shown), indicating little temperature dependence in the absorbance. This avoids the problem of simulation at 78 K where the force fields are not benchmarked.

dx.doi.org/10.1021/jp200553d |J. Phys. Chem. A XXXX, XXX, 000–000

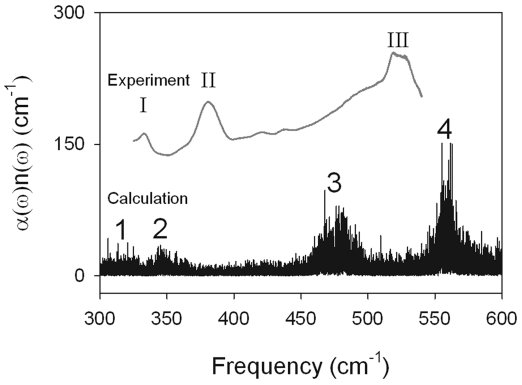

Figure 5. Comparison of calculated IR spectrum with experimental result for peptide AK17 (black, Arabic numerals). The 100 mM aqueous spectra of AK17 (dark gray, Roman numerals) is shown for band assignment purposes.

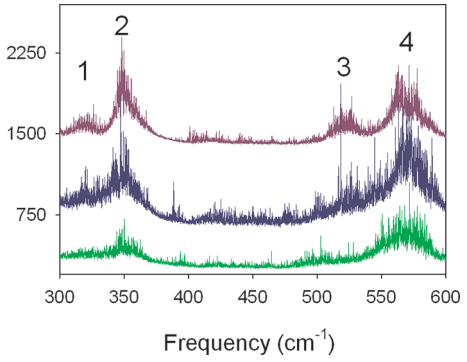

Figure 6. VDOS calculated from atomic velocity trajectories of 1 ns MD simulation: purple, AK17; blue, AK10G; green, AK9P. The VDOS of AK17 and AK10G spectra are offset for clarity by 750 units.

The calculated IR spectrum of AK17 generated from 1 ns of MD simulation was compared to the experimental IR spectrum (Figure 5). The four IR absorption bands generated by the simulation between 300 and 600 cm^{-1} (denoted 1−4) represent the calculated IR active vibrational modes. Among these four simulation bands, simulation band 1 centered at approximately 320 cm^{-1} is tentatively assigned to band I and simulation band 2 centered at approximately 350 cm^{-1} is tentatively assigned to band II. The assignment of simulation band 3 is ambiguous as it does not correspond easily with an observable band in the experimental data. It is possible this band is lost in the rising baseline seen in the experimental data or it is an artifact of the MD simulation. We propose that band III can be assigned to simulation band 4 (discussed later in the paper). The simulated IR spectra of all three peptides (Supporting Information) confirmed the IR active mode band 4 and supported the theory that the IR active modes, bands 1 and 2, diminished in peptides with less α-helical content. However, the noise levels for the less structured peptides (AK10G and AK9P) were much higher than for AK17, compromising the value of this interpretation.

MD simulation of the IR absorption spectrum provided a direct way to compare theoretical and experimental approaches, and illustrated that both methods reveal absorbance bands in the region of interest.[34] For interpretation of the spectral features, further decomposition of the spectra was needed. This was achieved

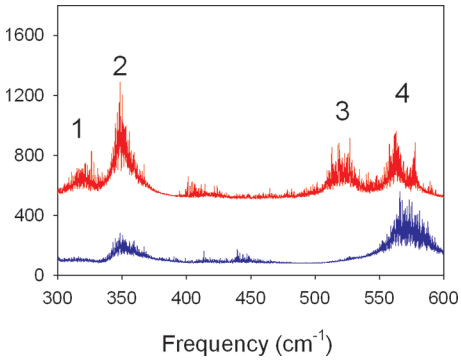

Figure 7. VDOS for AK17 backbone atoms (red) and side chain atoms (blue), the intensity of backbone spectrum is offset for clarity by 400 units.

by calculating the vibrational density of states (VDOS). VDOS represents all the vibrational modes in a molecule. It is worth noting that only some of the VDOS modes are infrared active. The advantage of VDOS is that it can be decomposed into contributions of each atom, which allow assignment of IR active bands to collective molecular motions.[34]

MD simulations were performed for all three peptides (AK17, AK10G, and AK9P) using the same conditions applied to AK17. Prior to the sampling period, AK17 retained its α-helical structure, whereas AK10G had a partially deformed helix and AK9P adopted a random coil configuration.[33] A comparison of the three VDOS generated from these three simulations (Figure 6) demonstrated a clear difference between VDOS for each peptide. For AK17, a clear one to one relation for bands 1, 2, and 4 between the calculated IR spectrum and VDOS was obtained, indicated by the same band notation in Figures 5 and 6. In the frequency region of 300−600 cm^{-1}, although very similar overall line shape for the two peptide spectra is shown, we observed a diminished vibrational spectrum density in simulation bands 1−3 from the helical AK17 to the random coil model (AK9P), while simulation band 4 shows very similar absorbance in all three peptides.

Figure 7 shows decomposed spectra of AK17, derived from the VDOS of backbone atoms and VDOS of side chain atoms. VDOS simulation band 1 (with a frequency that corresponds closely to band 1 in the simulated IR spectrum) is closely associated with peptide backbone vibrational modes and has no contribution from the peptide side chain. VDOS simulation band 2 (with a frequency that corresponds closely to band 2 in the simulated IR spectrum) has a contribution from both the peptide backbone and side chain. VDOS simulation band 3 frequency does not correspond with a band in the simulated IR spectrum and is assumed to be IR inactive. VDOS simulation band 4 (with a frequency that corresponds closely to band 4 in the simulated IR spectrum), like band 2, has a contribution from both the peptide backbone and side chain. It is worth noting that the VDOS simulation of the peptide AK9P (Figure 6) and the AK17 side chain (Figure 7) are very similar, indicating that there are no vibrational modes associated with in the peptide backbone in the random coil configuration in this part frequency range.

4. DISCUSSION

4.1. Aqueous versus Lyophilized Sample Preparation. The presentation of peptide as frozen aqueous samples sandwiched between polyethylene sheets, as opposed to dried (lyophilized)

dx.doi.org/10.1021/jp200553d |J. Phys. Chem. A XXXX, XXX, 000–000

samples pressed in polyethylene pellets, has a major negative consequence in that the ice absorbance prevents analysis of the peptide between 150 and 325 cm^{-1} and beyond 540 cm^{-1}. This is offset by the fact that lyophilization of a peptide sample may be accompanied by structural modification of the peptide as the protective solvation shell is removed, the secondary structure is compromised and there is also the possibility of higher-order structure formation such as crystallization or β-pleated sheeting. The spectra for AK17 does show a distinct red shift of bands I and II due to lyophilization (Figure 3B) which may be indicative of secondary structural change. The spectra of AK9P for aqueous and lyophilized samples are radically different. The band at 440 cm^{-1} in the lyophilized samples (Figure 3A) is well documented for dry preparations of β-sheet L-polyalanine.[13,35] The lyophilization process can introduce structural changes, such as β-sheet formation,[17] which is an undesired artifact when using far-infrared spectrometry for structural analysis of peptides or proteins. This finding justified the choice of an aqueous sample preparation over lyophilized peptide samples. By maintaining an aqueous environment the peptide conformation is more likely to be retained and artifacts arising from the lyophilization process are avoided.

4.2. Computational Studies. The far-IR spectra (between 50 and 600 cm^{-1}) of complex biomacromolecules are relatively poorly understood. This region is thought to be inhabited by primary vibrational modes within the peptide backbone, torsional modes of entities like methyl groups and possible ensembles of low-frequency resonances across the macromolecule. MD simulation is able to capture time-averaged molecular properties that approach the experimentally measurable ensemble averages. Previous research suggests that MD based methods are capable of quantitatively depicting the IR spectra of ambient water above 300 cm^{-1}[36] and has been applied to water bound to proteins.[37] The experimental spectra of AK17 in its frozen aqueous form and lyophilized dry form were similar so successive calculations of the IR spectrum of the three peptides focused on the peptide molecule without the presence of water. Good agreement was observed between experimental data and calculated IR spectra for the position of bands I and II. The small shift in frequency justified the choices of parameters used in the MD simulation. Simulation band 3 was not observed in the experimental data, its prominence in the simulation indicates that it is unlikely to be hidden in the rising baseline and should be considered to be an artifact in the simulation. Artifacts of MD simulation have been observed elsewhere and their cause is unclear.[37] Band 4 was assigned to experimental band III based on the VDOS simulation.

Further interpretations of the spectral features were made on the basis of VDOS generated by the same MD trajectories. Illustrated in Figure 6, the comparison of VDOS of an α-helical model (AK17) and random coil model (AK9P) further confirmed the structural dependence of vibrational spectrum in this frequency range of interest. From AK17 to AK9P, the decrease in vibrational spectrum density in simulation bands 1 and 2 correspond well to the experimental data. Further decomposition of the VDOS of simulation bands 1 and 2 revealed the predominant contribution from the peptide backbone, and the vibrational modes were more focused in the ordered structure of AK17 and dispersed in the random coil structure of AK9P.

The experimentally observed band III had a double peaks structure for lyophilized samples of AK17 and AK10G, whereas AK9P with its possible β-pleated structure had a discrete single peak (Figure 3A). This observation suggests the assignment of band III to VDOS simulation band 4 can be made on the basis that the observed resonance in the AK9P spectrum has lost the contribution from the peptide backbone and only the contribution from the side chain remains (Figure 7), a phenomenon in common with VDOS simulation band 4. It is also evident that backbone related bands (e.g., bands I and II) were substantially diminished. The double peak structure for band III seen in the experimental spectra among the three peptides in solution (Figure 2) further indicates that the β-sheet in lyophilized AK9P was not present in frozen aqueous AK9P. Furthermore, similar vibrational spectral intensities shown in simulation band 4 of VDOS across the three peptides agree with aqueous spectra well, supporting the band assignment we made here. Our results also agree well with the assignments of vibrational modes for poly alanine carried out by Lee et al.,[32] except the C_β bending that is assigned to a band at 328 cm^{-1} is not seen in our side chain VDOS.

4.3. Peptide Spectrum. Although the three peptides only differ by one amino acid in their sequence, they displayed vastly different secondary structure in solution, measured by circular dichroism spectroscopy (Table 1). The peptide band I (Figures 2 and 4) peak height progressively diminished from AK17 to AK9P, which corresponds with the decrease in helicity of the peptides (Table 1). The transition from a defined band in AK17 to very weak band absorbance seen in the random coil peptide AK9P suggests the dominance of structural related vibrational mode(s) in this band. For band II of the aqueous peptide (Figures 2 and 4), a clear separation can also be observed between the random coil peptide AK9P and the other two peptides with helical content, in terms of both peak height and frequency. In contrast to band I, a residual amount of peak height remains for AK9P, suggesting only part of the modes contributing to this band are structurally dependent. AK9P shows no helix content in the CD measurement, indicating a less-ordered conformation. Therefore, coupled backbone vibrational modes of amino acids of the less-ordered conformation will be more widely spread in the frequency domain, which could result in the diminished band absorbance seen in bands I and II.

In earlier polypeptide studies,[13,38] a weak band at 325−328 cm^{-1} and a strong band at 372−374 cm^{-1} were reported for α-helical conformation of polyalanine, which correspond to bands I and II in this study. These earlier studies investigated crude mixtures of peptides with variable chain lengths. The work presented here used very well-defined synthetic polypeptide chains of exactly 17 amino acids. The well reproduced frequencies in bands I and II for mixed length polyalanine indicates that the vibrational modes do not correspond to large scale molecular motions but are associated with the secondary structure of the peptide backbone.

4.4. Conclusion. The relative transparency of ice between 325 and 540 cm^{-1} enables frozen aqueous biological samples to be studied within this bandwidth. Previous analysis using far-infrared spectroscopy relied on the removal of water from the sample to minimize the water absorbance. In this work, we capture vibrational modes of peptides in the frozen aqueous state, which is closer to the environment under physiological aqueous conditions than a lyophilized sample. It can avoid the conformational changes caused by dehydrating the samples. In the case of AK9P, this was observed as a loss of bands I and II and the emergence of a band at 440 cm^{-1} was probably associated with the formation of a β-pleated structure.

Experimental analysis and the VDOS simulation of the three alanine-rich peptides with differing secondary structure indicated

that there are three distinct modes between 325 and 540 cm^{-1}. Band I is clearly associated with vibrations in the peptide backbone when in the α helix conformation. Band II is association with the peptide backbone, diminishes with reduction in helicity and is lost altogether on β-sheet formation. Band III differs in having both a peptide backbone and side chain vibrational modes. When bands I and II are used as fingerprint resonances, the method presented in this paper could be used to study the secondary structure of polypeptides in environments that may not be accessible by other methods.

■ ASSOCIATED CONTENT

Supporting Information. The calculated IR spectrum of AK17, AK10G, and AK9P. This material is available free of charge via the Internet at http://pubs.acs.org.

■ AUTHOR INFORMATION

Corresponding Author

*Tel.: +441142227500. Fax +441142227501. E-mail: r.j.falconer@sheffield.ac.uk.

■ ACKNOWLEDGMENT

This work was funded by the Australian Research Council grant number DP0773111 and supported by the National Collaborative Research Infrastructure Strategy, an Australian Federal Government initiative. T.H. thanks the Australian Research Council for a Future Fellowship. We thank the Australian Synchrotron for access to their infrared beamline (Grant Nos. FI1137 and FI1437), and Dominique Appadoo and Danielle Martin of the Australian Synchrotron for their assistance.

■ REFERENCES

(1) Provencher, S. W.; Glockner *J. Biochem.* **1981**, *20*, 33–37.
(2) Sreerama, N.; Woody, R. W. *Anal. Biochem.* **2000**, *287*, 252–260.
(3) Byler, D. M.; Susi, H. *Biopolymers* **1986**, *25*, 469–487.
(4) Jackson, M.; Mantsch, H. H. *Crit. Rev. Biochem. Mol. Biol.* **1995**, *30*, 95–120.
(5) Lippert, J. L.; Tyminski, D.; Desmeules, P. J. *J. Am. Chem. Soc.* **1976**, *98*, 7075–7080.
(6) Williams, R. W. *J. Mol. Biol.* **1983**, *166*, 581–603.
(7) Itoh, K.; Shimanouchi., T. *Biopolymers* **1965**, *5*, 921–930.
(8) Abe, Y.; Krimm, S. *Biopolymers* **1972**, *11*, 1817–1839.
(9) Abe, Y.; Krimm, S. *Biopolymers* **1972**, *11*, 1841–1853.
(10) Moore, W. H.; Krimm, S. *Biopolymers* **1976**, *15*, 2439–2464.
(11) Moore, W. H.; Krimm, S. *Biopolymers* **1976**, *15*, 2465–2483.
(12) Itoh, K.; Nakahara, T.; Shimanou., T; Oya, M.; Uno, K.; Iwakura, Y. *Biopolymers* **1968**, *6*, 1759–1766.
(13) Buontempo, U.; Careri, C.; Fasella, P.; Ferraro, A. *Biopolymers* **1971**, *10*, 2377–2386.
(14) Falconer, R. J.; Zakaria, H.; Fan, Y. Y.; Bradley, A. P.; Middelberg, A. P. J. *Appl. Spectrosc.* **2010**, *64*, 1259–1264.
(15) Zakaria, H.; Jones, I.; Fischer, B. M.; Abbott, D.; Middelberg, A. P. J.; Falconer, R. J. *Appl. Spectrosc.* **2011**, *65*, 260–264.
(16) Png, G. M.; Falconer, R. J.; Fischer, B. M.; Zakaria, H. A.; Mickan, S. P.; Middelberg, A. P. J.; Abbott, D. *Opt. Express* **2009**, *17*, 13102–13115.
(17) Griebenow, K.; Klibanov, A. M. *Proc. Natl. Acad. Sci. U.S.A.* **1995**, *92*, 10969–10976.
(18) Dong, A. C.; Prestrelski, S. J.; Allison, S. D.; Carpenter, J. F. *J. Pharm. Sci.* **1995**, *84*, 415–424.
(19) Guillot, B. *J. Chem. Phys.* **1991**, *95*, 1543–1551.
(20) Silvestrelli, P. L.; Bernasconi, M.; Parrinello, M. *Chem. Phys. Lett.* **1997**, *277*, 478–482.
(21) Gaigeot, M. P.; Sprik, M. *J. Phys. Chem. B* **2003**, *107*, 10344–10358.
(22) van Gunsteren, W. F.; Bakowies, D.; Baron, R.; Chandrasekhar, I.; Christen, M.; Daura, X.; Gee, P.; Geerke, D. P.; Glattli, A.; Hunenberger, P. H.; Kastenholz, M. A.; Ostenbrink, C.; Schenk, M.; Trzesniak, D.; van der Vegt, N. F. A.; Yu, H. B. *Angew. Chem., Int. Ed.* **2006**, *45*, 4064–4092.
(23) Car, R.; Parrinello, M. *Phys. Rev. Lett.* **1985**, *55*, 2471–2474.
(24) Greenfield, N. J.; Hitchcock-Degregori, S. E. *Protein Sci.* **1993**, *2*, 1263–1273.
(25) Hirschfeld, T.; Mantz, A. W. *Appl. Spectrosc.* **1976**, *30*, 552–553.
(26) Eswar, N.; Webb, B.; Marti-Renom, M. A.; Madhusudhan, M. S.; Eramian, D.; Shen, M.-Y.; Pieper, U.; Sali, A. *Comparative Protein Structure Modeling Using MODELLER*; Wiley: Hoboken, NJ, 2007; Unit 2.9.
(27) Berendsen, H. J. C.; Postma, J. P. M.; van Gunsteren, W. F.; Hermans, J. *Intermolecular Forces*; D. Reidel Publishing Company: Dordrecht, Germany, 1981.
(28) Schuler, L. D.; Daura, X.; Van Gunsteren, W. F. *J. Comput. Chem.* **2001**, *22*, 1205–1218.
(29) McQuarrie, D. A. *Statistical Mechanics*; Harper-Collins Publishers: New York, 1976.
(30) Berens, P. H.; Mackay, D. H. J.; White, G. M.; Wilson, K. R. *J. Chem. Phys.* **1983**, *79*, 2375–2389.
(31) Warren, S. G. *Appl. Opt.* **1984**, *23*, 1206–1225.
(32) Lee, S. H.; Krimm, S. *Biopolymers* **1998**, *46*, 283–317.
(33) Ding, T.; Li, R.; Zeitler, J. A.; Huber, T .L.; Gladden, L. F.; Middelberg, A. P. J.; Falconer, R. J. *Opt. Express* **2010**, *18*, 27431–27444.
(34) Gaigeot, M. P.; Martinez, M; Vuilleumier, R. *Mol. Phys.* **2007**, *105*, 2857–2878.
(35) Fanconi, B. *Biopolymers* **1973**, *12*, 2759–2776.
(36) Madden, P. A.; Impey, R. W. *Chem. Phys. Lett.* **1986**, *123*, 502–506.
(37) Woods, K. N. *Phys. Rev. E* **2010**, *81*, 031915.
(38) Dwivedi, A. M.; Krimm, S. *Biopolymers* **1984**, *23*, 923–943.